
Online Edge Grafting for Efficient MRF Structure Learning

Walid Chaabene

Department of Computer Science
Virginia Tech
Blacksburg, VA 24060
walidch@vt.edu

Bert Huang

Department of Computer Science
Virginia Tech
Blacksburg, VA 24060
bhuang@vt.edu

Abstract

Incremental methods for structure learning of pairwise Markov random fields (MRFs), such as *grafting*, improve scalability to large systems by avoiding inference over the entire feature space in each optimization step. Instead, inference is performed over an incrementally grown active set of features. In this paper, we address the computational bottlenecks that current techniques still suffer by introducing *online edge grafting*, an incremental, structured method that activates edges as groups of features in a streaming setting. The framework is based on reservoir sampling of edges that satisfy a necessary activation condition, approximating the search for the optimal edge to activate. Online edge grafting performs an informed edge search set reorganization using search history and structure heuristics. Experiments show a significant computational speedup for structure learning and a controllable trade-off between the speed and the quality of learning.

1 Introduction

A powerful family of approaches for learning the structure of Markov random fields (MRFs) is based on minimizing ℓ_1 -regularized scores such as the negative log likelihood [2] of a fully connected MRF. The regularization reduces the parameters of irrelevant edges to zero. The main challenge when using these methods is that, for large enough MRFs, the feature space becomes extremely large and causes an overwhelmingly high computational cost. Active-set methods, such as grafting [8, 14], were introduced to promote more scalability. Despite the benefits of active-set learning, grafting retains significant computational costs: As a mandatory pre-learning step, grafting requires computing sufficient statistics of all possible variable pairs to enable greedy activation tests on the entire search space, and each iteration of grafting requires a search over the entire combinatorial space of all possible edges. Furthermore, grafting does not reason about the MRF graph structure, activating a single parameter at a time.

This paper introduces *online edge grafting*, an active-set method that activates edges in an online fashion as groups of parameters. We derive an edge-activation test using a structured group- ℓ_1 learning objective. The edge search space is stored in a min-heap priority queue [15] where edges are assigned different search priorities. The method performs online edge activation using a control sample of candidate edges stored in a limited-memory reservoir. Search priorities are updated based on the search history and structural information derived from the partially constructed MRF structure learned so far. The framework provides high scalability since it allows on-demand computation of sufficient statistics for edges that are likely to be activated. This strategy eliminates the heavy computation of the grafting’s pre-learning phase, enabling online edge grafting to start—and even finish in some cases—learning well before grafting is able to begin learning. We also introduce a trade-off parameter to balance the speed of learning and the quality of learned MRFs.

Our experiments show that online edge grafting scales better to large datasets than grafting. Synthetic experiments show that the proposed method performs well at recovering the true structure, while real data experiments show that we obtain high quality learned MRFs on large and diverse datasets.

2 Background

Throughout this paper, we consider the case of log-linear, pairwise Markov random fields (MRFs). Based on a given MRF structure, the probability of a set of variables $x = \{x_1, \dots, x_n\}$ is $p_w(x) = \frac{1}{Z(w)} \prod_{c \in C} \phi_c(x; w)$, where $Z(w)$ is a normalizing partition function $Z(w) = \sum_x \prod_{c \in C} \phi_c(x; w)$, and ϕ is a clique potential function $\phi_c(x; w) = \exp(\sum_{k \in c} w_k f_k(x))$. The set C contains indices representing cliques and variables, and $f_k(x)$ are feature functions often defined as indicator functions. In the case of pairwise Markov random fields, a clique can either refer to a node or an edge. A pairwise MRF is associated with an undirected graph $G(V, E)$, where V is the set of n nodes corresponding to variables, and E is the set of edges corresponding to pairwise cliques. The factorization for a pairwise MRF is $p_w(x) = \frac{1}{Z(w)} \prod_{i \in V} \phi_i(x; w) \prod_{(i,j) \in E} \phi_{ij}(x; w)$.

2.1 Parameter learning through ℓ_1 -regularized likelihood

Given a set of data $X = \{x^{(m)}\}_{m=1 \dots N}$, the likelihood is expressed as $l(w) = \frac{1}{N} \prod_{m=1}^N p_w(x^{(m)})$. A high likelihood $l(w)$ reflects the model's ability to represent and predict data. For numerical stability, we formulate learning as a minimization of a negative log likelihood $L(w)$, where

$$L(w) = -\frac{1}{N} \sum_{m=1}^N \log p_w(x^{(m)}) = -\frac{1}{N} \sum_{m=1}^N (w^\top f(x^{(m)})) + \log Z(w), \quad (1)$$

and w and f correspond to the vectors of w_k and f_k , respectively. Minimizing $L(w)$ is often done using gradient-based methods. The gradient of $\log Z(W)$ with respect to the k^{th} feature is the model's expectation of the k^{th} feature function [6]: $\frac{\partial \log Z}{\partial w_k} = E_w[f_k(x)] = \sum_x p_w(x) f_k(x)$. Therefore, the gradient of L with respect to the k^{th} feature is

$$\frac{\partial L}{\partial w_k} = -\frac{1}{N} \sum_{m=1}^N f_k(x^{(m)}) + E_w[f_k(x)] = E_w[f_k(x)] - E_D[f_k(x)] := \delta_k L. \quad (2)$$

In other words, the feature-wise gradient $\delta_k L$ is the error between the data expectation E_D and the model expectation E_w of $f_k(x)$. The goal of learning can be seen as minimizing that error. To avoid over-fitting and to promote sparsity of the learned weights and of the learned Markov network, classical methods add an ℓ_1 regularization and solve $\min_w L(w) + \lambda \|w\|_1$.

2.2 Learning challenges

Despite the clarity of its expression, the computation of the gradient is prohibitively expensive: (i) The data expectation requires the computation of sufficient statistics for every unary and pairwise feature. These are significant computations, especially for large datasets. (ii) The classical ℓ_1 formulation ignores the structure of MRFs and treats parameters independently. This treatment dismisses the importance of local consistencies and the intrinsic identity of each variable and each edge. Finally, (iii) inference of the model expectations $E_w[f_k(x)]$ is generally #P-complete [6].

The main focus of existing techniques has been on minimizing the cost of the inference subroutine (iii). Active-set methods aim to allow the learning optimization to compute inference over simpler MRFs. And various approximate inference methods can efficiently compute approximate expectations, such as loopy belief propagation and its variants [5, 7, 10, 11, 13, 16]. Our proposed work addresses the first two challenges of sufficient statistics computation (i) and structure coherence (ii).

2.3 Grafting

Grafting [8, 14] is an active-set approach for learning that alternates between two primary operations: (1) It learns parameters for an active set S of features (e.g., using a sub-gradient method); And (2)

it expands the active set by activating one feature using a gradient test. The gradient test is based on the Karush-Kuhn-Tucker (KKT) conditions of the ℓ_1 -regularized objective. Grafting converges when the activation step does not find any new feature or when a predefined maximum number of features f_{\max} is reached. Grafting has a startup bottleneck with an $O(n^2 N s_{\max}^2)$ computational cost to compute the sufficient statistics for each feature, for a system of n variables and a maximum number of states s_{\max} . In addition, grafting performs an exhaustive, $O(n^2 s_{\max}^2)$ -complexity search to activate one feature. These bottlenecks translate to poor scalability for large systems and datasets.

A variant called *grafting-light* [17] is a faster extension of grafting, which aims to reduce the computational cost of optimization by running one orthant-wise gradient step each time a new feature is selected. Although this method produces a faster optimization step, it does not address the cost of exhaustive activation tests and is more likely to produce a high number of irrelevant active features, yielding slower learning and a stronger risk of over-fitting.

Although grafting and grafting-light are fairly suitable for learning MRFs, they do not consider structural information and do not consider different clique-memberships of features. Furthermore, grafting methods require computing the sufficient statistics for each feature in the search space before even activating the first feature. This operation requires an $O(n^2 N s_{\max}^2)$ cost, which is prohibitively expensive for large-scale datasets. We address these issues in the proposed method.

3 Online Edge Grafting

We propose *online edge grafting*, a method that grafts edges—as opposed to features—in an online fashion using a variation of reservoir sampling [12]. This method is online in that it activates edges without considering the entire search space, and it performs edge grafting in that it activates entire edges as groups of parameters.

Online edge grafting computes statistics on-demand within the learning loop, and it reorganizes the search space by assigning search priorities to edges based on search history and structure information derived from the partially constructed MRF graph. The goal is to prioritize testing of edges that are more likely to be relevant. We first introduce the exhaustive variant of our approach and then introduce the online activation mechanism.

3.1 Exhaustive edge grafting

Our first extension to classical, feature-based grafting encodes structural information into the objective function. We refer to this variation as *edge grafting*, which is the exhaustive version of our proposed online method. Edge grafting activates edges instead of features. Accordingly, we redefine the search set F and the active set S respectively as sets of inactive and active edges.

To include structural information in the likelihood function, we use the group- ℓ_1 formulation. In doing so, the learned parameters of each node and each edge tend to be homogeneous, and whole edges tend to be sparse. We define the group- ℓ_1 negative log likelihood as follows:

$$\mathbb{L}(w) = L(w) + \sum_{g \in G} \lambda d_g \|w_g\|_2 + \lambda_2 \|w\|_2^2. \quad (3)$$

A group g can either refer to a node or an edge. Consequently, w_g refers to the sub-vector containing all weights related to features of group g . We define d_g as the number of states per clique. As in elastic-net methods [18], we add the ℓ_2 -norm to avoid some shortcomings of group- ℓ_1 regularization such as parameter imbalance and aggressive group selection.

We derive a similar KKT optimality condition to group regression [9] as follows:

$$\begin{cases} \frac{\|\delta_g L\|_2}{d_g} + \lambda_2 \|w_g\|_2^2 = 0 & \text{if } \|w_g\|_2 \neq 0 \\ \frac{\|\delta_g L\|_2}{d_g} \leq \lambda & \text{if } \|w_g\|_2 = 0, \end{cases} \quad (4)$$

where $\delta_g L$ is the sub-vector constructed using the entries of the gradient vector L corresponding to group g . From this condition, we derive an edge-activation test for a given edge $e \in F$,

$$C_2 : s_e > \lambda, \quad (5)$$

where s_e is the activation score representing the error between the model $\hat{p}_w(e)$ and the data $p_D(e)$,

$$s_e = \frac{\|\delta_e L\|_2}{d_e} = \frac{\|\hat{p}_w(e) - p_D(e)\|_2}{d_e}. \quad (6)$$

By using the group- ℓ_1 regularizer and maintaining an active set of edges, edge grafting operates analogously to grafting, except it activates the parameters for entire edge potentials at once. The group- ℓ_1 formulation for edges allows the sparsity to be consistent with graph structure and intuitions about variable independence in MRFs. We summarize edge grafting, as discussed in Section 3.1, in Algorithm 1.

Algorithm 1 Edge Grafting

```

1: Define EdgeNum as the maximum allowed number of edges to graft
2: Initialize  $E = \emptyset$  and  $F =$  set of all possible edges
3: Compute sufficient statistics of  $e \forall e \in F$  # cost:  $O(n^2 N s_{\max}^2)$ 
4: AddedEges = 0
5: Continue = True
6: while EdgeNum > AddedEges and Continue do
7:   Compute score  $s_e \forall e \in F$  # cost:  $O(n^2 s_{\max}^2)$ 
8:    $e^* = \arg \max_{e \in F} s_e$ . # cost:  $O(n^2)$ 
9:   if  $s_{e^*} > \lambda$  then
10:     $E = E \cup \{e^*\}; F = F \setminus \{e^*\}$ 
11:    AddedEges = AddedEges + 1
12:    Perform optimization over new active set
13:   else
14:     Continue = False
15:   end if
16: end while

```

With these improvements, edge grafting addresses one shortcoming of using classical grafting for MRF structure learning. However, it still requires compute sufficient statistics for all possible edges and having to search over all possible edges at each iteration. Next, we introduce our full, proposed approach that addresses these bottlenecks.

3.2 Online edge grafting using reservoir sampling

Edge grafting results in fewer activation and optimization iterations than grafting since it activates groups of parameters rather than edge features. However, it still suffers major bottlenecks, having to compute sufficient statistics for all possible edges and having to perform activation tests for all edges at each iteration. Each of these operations has an $O(n^2)$ computational cost. To address these bottlenecks, we derive *online edge grafting*, which activates edges without exhaustively computing all sufficient statistics or performing all activation tests. Instead, the approach starts activating edges by computing a small fraction of the edge sufficient statistics. A naive strategy for online activation would be to activate the first encountered edge that satisfies C_2 . However, this approach can introduce a large number of spurious edges. We propose an adaptive approach inspired by *best-choice problems* that uses a control sample of edges satisfying C_2 , stored in a limited-memory reservoir R . By maintaining a reservoir of potential edges to activate, we increase the probability of the algorithm activating relevant edges.

The overall method is summarized as follows. The algorithm first initializes a min-heap priority queue [15] of all possible edges. The main learning loop then extracts edges from the priority queue and places any edges that pass the activation test into the reservoir, retaining the edges that violate the optimality condition the most in the reservoir. Once enough edges have been seen, the algorithm selects non-adjacent edges from the reservoir to activate and then performs inference to update the model expectations. The priority queue is then updated based on the newly estimated MRF structure, and the next iteration of the main loop begins.

There are no quadratic-time operations within the main loop of the algorithm, and the only quadratic-time operation is the initialization of the priority queue, which could be replaced with a random-sampling approach for unseen edges. Even though there are $O(n^2)$ elements in the priority queue,

each insertion, removal, or update operation costs time logarithmic in the number of stored elements, which is $O(\log(n^2)) = O(2\log(n)) = O(\log(n))$. The logarithmic cost eliminates the dependency on quadratic-time operations, enabling the prioritization and management of the large search space. We detail the specific strategies of the various phases in the remainder of this section.

3.2.1 Reservoir management

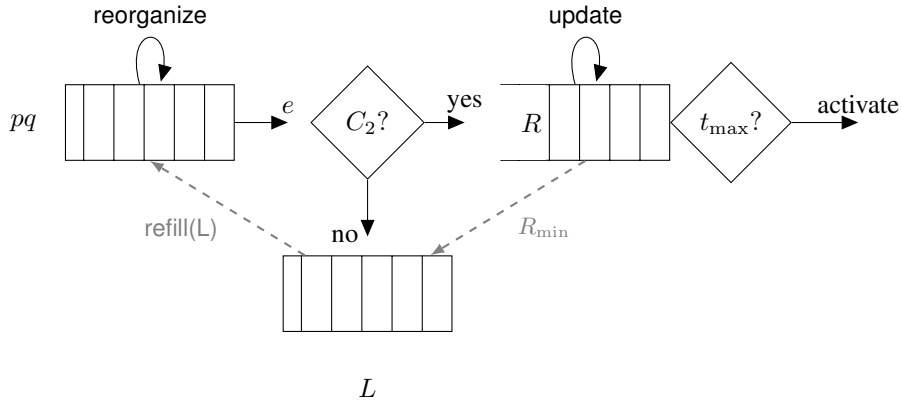
Online edge grafting uses some strategies to influence the reservoir of potential edges to activate in order to contain edges that are likely to be relevant. Let $A \in F$ be the unknown set of all edges that satisfy C_2 at an activation iteration. We construct a control sample $R \subseteq A$ from which we activate edges using a confidence interval. In the first activation iteration, the search set F is stored in a min-heap priority queue with equal priorities. Then, we parse through the priority queue by extracting one edge at a time, generating a prioritized stream of edges to test. If a tested edge satisfies C_2 , it gets added to R . Otherwise, it gets ignored.

When a maximum number of edge tests t_{\max} is reached, we start activating edges. To maintain a high-quality reservoir, edge activation only starts after we fill R to capacity in the first edge activation iteration. Furthermore, if R reaches its capacity before t_{\max} is reached, we replace the minimum-scoring edge in R with the newly tested edge whenever it has a higher score. We use a simple strategy to activate edges in the reservoir with high activation scores where we consider edges that have at least an above-average score. We compute the average activation score $\mu = \frac{1}{|R|} \sum_{e \in R} s_e$, and then we define a confidence interval for choosing edges that are likely to be relevant as $I_\alpha = [\mu + \alpha(\max_{e \in R} s_e - \mu), \max_{e \in R} s_e]$, where $\alpha \in [0, 1]$. The algorithm considers activating edges with activation scores no less than $\tau_\alpha = (1 - \alpha)\mu + \alpha \max_{e \in R} s_e$. After deriving τ_α , edges are activated in a decreasing order with respect to their scores. To avoid redundant edges and to promote scale-free structure, we only activate edges that are not adjacent. Note that when $\alpha = 1$, we only select the maximum-scoring edge. Reducing α increases the number of edges to be activated at a certain step but can also result in adding spurious edges. In our experiments, we show the impact of different values of α on the quality of the learned MRFs and convergence speed.

After each optimization step, edge gradients change. Therefore, scores of reservoir edges are updated, and edges that no longer satisfy C_2 are dropped from the reservoir.

Figure 1 presents a high-level description of the online edge-activation mechanism.

Figure 1: High-level operational scheme of the edge activation mechanism. From left to right, the first structure is the priority queue (pq) initialized with the set of all possible edges. The next diamond-shaped box represents the activation test C_2 , after which an edge is either added to the reservoir (R) or to the frozen edge container L . The t_{\max} box represents when the maximum number of edge tests is reached, after which edges are activated. The gray, dashed line on the right (R_{\min}) indicates the injection of the minimum scoring edge in R into L , when R is full. The gray dashed line on the left ('refill()') indicates refilling the priority queue when it is emptied with the frozen edges.



3.2.2 Search space reorganization

Search space reorganization is performed by assigning and updating the search priority of edges in the priority queue. The aim of this reorganization is to increase the quality of the received stream of edges and to increase the reservoir quality. We leverage search history and structural information.

Search history At a given activation iteration, an edge with a small activation score is unlikely to satisfy C_2 in the future and is placed further toward the tail of the priority queue. We define an edge violation offset $v_e = 1 - \frac{s_e}{\lambda}$. When the activation tests fail or edges are dropped from R , the low-score edges are not immediately returned to the priority queue but instead placed, along with their violation offsets, in a separate container L . We refer to such edges as “frozen” edges. When the search priority queue is emptied, we refill it by re-injecting frozen edges from L with their respective violation offsets as their new priorities.

Partial structure information As the active set grows, so does the underlying MRF graph G . The resulting partial structure contains rich information about dependencies between variables. We rely on the hypothesis that graphs of real networks have a scale-free structure [1]. We therefore promote such structure in the learned MRF graph by encouraging testing of edges incident to central nodes.

We start by measuring node centrality on the partially constructed MRF graph G to detect hub nodes. A degree-based node centrality c_i for a node i is the fraction of all possible neighbors it is connected to, $c_i = \frac{|N_i|}{|V|-1}$. We then use a centrality threshold \hat{c} to identify the set of hubs $H = \{i \in V \text{ such that } c_i > \hat{c}\}$. Finally, we prioritize all edges that are incident to nodes in the set H by decrementing their min-heap value by 1.0. The total cost of updating the priority queue is $O(|H|n \log(n))$, where $O(\log(n))$ represents the cost of updating the priority of an edge in the min-heap structure.

Reorganizing the priority queue pushes edges that have a higher chance of being relevant to the front of the priority queue. The reorganization encourages a higher-quality reservoir and activates higher-quality edges at each activation iteration.

The priority-queue reorganization subroutine is summarized in Algorithm 2.

Algorithm 2 Reorganize PQ

- 1: Compute centrality measures over partially constructed MRFs graph G
 - 2: Construct the hub set H # cost: $O(n)$
 - 3: **for** $h \in H$ **do**
 - 4: **for** $n \in V$ **do**
 - 5: $pq[(h,n)] = pq[(h,n)] - 1$ # total loop cost: $O(|H|n \log(n))$
 - 6: **end for**
 - 7: **end for**
-

The activation mechanism is presented in Algorithm 3.

Algorithm 3 Activation Test

```
1: Reorganize  $pq$  using Algorithm 2
2:  $E^* = \emptyset$ 
3:  $t = 0$ 
4: repeat
5:   if  $pq$  is empty then
6:     if  $R$  is empty then
7:       Break
8:     end if
9:      $pq = \text{Refill}(L)$ 
10:  end if
11:  Extract edge  $e$  with highest priority from  $pq$ 
12:  if Sufficient statistics of  $e$  not already computed then
13:    Compute sufficient stats of  $e$  # cost:  $O(Ns_{\max}^2)$ 
14:  end if
15:  Compute score  $s_e$ . # cost:  $O(s_{\max}^2)$ 
16:  if  $s_e > \lambda$  and  $R$  not full then
17:    Add  $e$  to  $R$  # add  $e$  if capacity not reached
18:  else if  $s_e > \lambda$  and ( $R$  is full and  $R_{\min} < s_e$ ) then
19:    Replace  $R_{\min}$  by  $e$ . #  $R_{\min}$ : minimum scoring edge in  $R$ 
20:    Place  $R_{\min}$  in  $L$ .
21:  else
22:    Place  $e$  in  $L$ 
23:  end if
24: until  $t = t_{\max}$ 
25: Compute  $\tau$ 
26: for  $e \in R$  s.t.  $s_e \geq \tau$  do
27:   if  $e$  not adjacent to edges in  $E^*$  then
28:      $E^* \cup \{e\}$ 
29:   end if
30: end for
```

We finally have all the pieces to construct the main online edge grafting framework in Algorithm 4.

Algorithm 4 Online Edge Grafting

```
1: Define EdgeNum as the maximum allowed number of edges to graft
2: Initialize  $E = \emptyset$ ,  $F =$  set all possible edges
3: Fill  $pq$  with all elements of  $F$  and assign equal priorities
4: AddedEges = 0
5: Fill  $R$  to capacity
6: while EdgeNum > AddedEges do
7:   Get set  $E^*$  of edges to activate using Algorithm 3
8:   if  $E^*$  is empty then
9:     Break
10:  end if
11:  for  $e^*$  in  $E^*$  do
12:     $E = E \cup \{e^*\}$ ;  $F = F \setminus \{e^*\}$ 
13:    AddedEges = AddedEges + 1
14:  end for
15:  Perform an optimization over active parameters.
16: end while
```

3.3 Complexity analysis

If it takes the algorithm r edge tests to fill the reservoir in one pass, then online edge grafting performs $\tilde{O}(rNs_{\max}^2)$ operations to compute the sufficient statistics necessary to fill the reservoir and activate the first edges. (We use \tilde{O} notation, omitting the logarithmic costs of using the priority

queue.) To activate the j^{th} edge, the algorithm needs to perform at most $\tilde{O}((r + jt_{\max})Ns_{\max}^2)$ operations, where t_{\max} is the allowed number of edge tests between two activation steps.

In the usual case, we assume that it takes the algorithm $r = O(|R|)$ tests to fill the reservoir R . Furthermore, to construct a relevant reservoir, we set $|R| = O(n)$. We also set $t_{\max} \ll n$, so to activate the j^{th} edge, the algorithm needs to compute at most $O((n + jt_{\max})Ns_{\max}^2)$ sufficient statistics tables. In the case of edge grafting, the algorithm needs to compute $O(n^2Ns_{\max}^2)$ to start grafting the first edge. Since $(n + jt_{\max}) \ll n^2$, our method provides a drastic speed up, as we circumvent the quadratic term in n and replace it with a linear term. It is worth noting that the priority-queue initialization has a complexity of $O(n^2 \log(n))$ for online edge grafting. This one-time cost does not scale with the number of training examples N , and it can be avoided by using random sampling of edges for unseen edges, rejecting edges that have been seen and prioritized, or using a hash-collision strategy to find a previously unseen edge when desired. For completeness, we include pseudocode for the discussed algorithms in the appendix.

4 Experiments

We perform experiments with both synthetic and real data on a Linux machine with 16 GB of RAM and a 3-GHz processor. For scalability analysis, we use datasets of varying variable dimensions and dataset sizes. In the synthetic setting, we simulate MRFs and generate data using a Gibbs sampler. In the real setting, we use three diverse datasets. Experiments using feature-based grafting proved to be extremely slow and would not fit well with methods in the edge-grafting family. Instead, our primary baselines are exhaustive edge grafting (labeled “EG” in figures) and online edge grafting with no reservoir (“first hit”), which activates the first edge that passes the edge-activation condition. We are interested in measuring the recovery of the true underlying graphical model structure as well as the ability of the learned MRF to model the data distribution. As a structure-recovery metric, we use recall, defined as the fraction of true edges recovered. We monitor recall over time. The slope of recall against time is an indicator of precision, as a high slope indicates that a method adds relevant edges and a small slope indicates the activation of several false-positive edges. We also measure the learning objective to compare how well each method optimizes. To measure how well the learned MRFs represent the true data distribution, we measure the pseudo-likelihood [3] of held-out test data.

4.1 Synthetic data

We construct random, scale-free-structured MRFs with variables having five states each. We generate preferential-attachment graphs [1] of size 50, 100, 200, and 400, with 30,875, 124,250, 498,500, and 1,997,000 parameters, respectively. We grow a graph by attaching new nodes each with two edges that are preferentially attached to existing nodes with high node centrality. The algorithm produces in $(2n - 4)$ edges. For each node and each created edge we sample their corresponding parameters from a Normal distribution with a mean equal to 100 and standard deviations $\sigma_v = 0.5$ (for nodes) and $\sigma_e = 1$ (for edges). This setting puts more emphasis on the edges (pairwise relationships between nodes) and helps avoid overfitting the model on the unary potentials.

We use grid search to detect the best combination of λ and λ_2 . We limit our search range to set $\{10^{-4}, 10^{-3}, 10^{-2}, 10^{-1}\}$ for λ and set $\{0.5, 1, 1.5\}$ for λ_2 . For each case we choose the pair (λ, λ_2) that produces the best recall and test NLPL for the baseline, *i.e.* edge grafting. It is worth noting that we did not notice a high sensitivity of the methods for different values of λ_2 , whereas smaller values of λ produces spurious edges for different methods.

We then use Gibbs sampling to generate a set of 20,000 data points, which we randomly split as training and held-out test data. We use grid search to tune the learning parameters. We fix $|R| = n$, and $t_{\max} \ll n$.

To generate data, we use Gibbs sampler to generate a set of 20,000 data points, which we randomly split as 19,000 training data points and 1,000 held-out testing data points.

We use grid search to detect the best combination of λ and λ_2 . We limit our search range to set $\{10^{-4}, 10^{-3}, 10^{-2}, 10^{-1}\}$ for λ and set $\{0.5, 1, 1.5\}$ for λ_2 . For each case we choose the pair (λ, λ_2) that produces the best recall and test NLPL for the baseline, *i.e.* edge grafting. It is worth

noting that we did not notice a high sensitivity of the methods for different values of λ_2 , whereas smaller values of λ produces spurious edges for different methods.

We first investigate the behavior of different methods when executed until no violating edge remains in the search space. We are interested in measuring the different methods' speeds of convergence and validating that they lead to similar solutions.

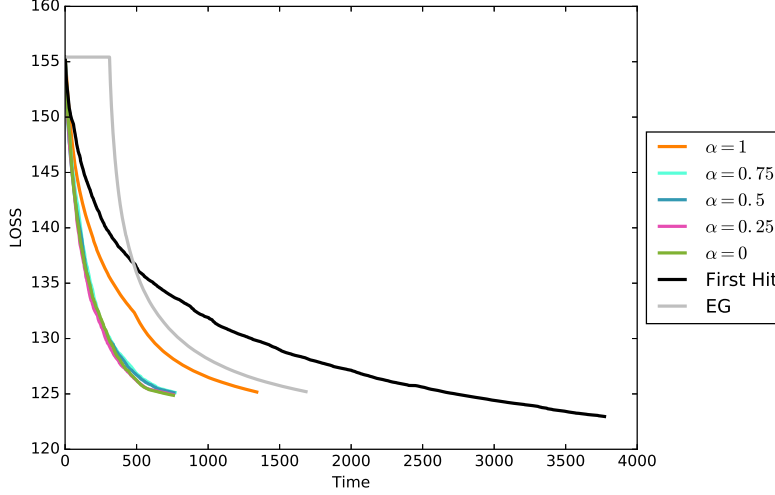


Figure 2: Objective values vs. seconds during full convergence of different methods (100 nodes). See the appendix for larger-size reproductions of these figures and additional plots.

Figure 2 shows that all methods appear to reach a similar minimum value of the objective function but with a faster convergence rate for online edge grafting. The first-hit baseline starts with a fast descent rate, but its activation of lower-violation edges eventually causes it to converge slower than edge grafting. Using a reservoir maintains a steep descent until convergence. These experiments also confirm that edge grafting suffers a major computational bottleneck of computing sufficient statistics, causing it to start optimization later than online edge grafting, after online edge grafting has nearly converged.

Figure 3 plots the recall of true edges over time. We fix the maximum number of edges that can be activated to be $3n$, stopping early when each algorithm exhausts this limit. For increasing values of α , we get better recall for different MRF sizes. However, this comes at the cost of a more expensive learning optimization. In fact, for smaller values of α , online edge grafting tends to activate more edges but with lower quality, which introduces a greater number of false-positive edges. We also observe that, for increasing amounts of variables, the learning gap between online edge grafting and exhaustive edge grafting increases, which demonstrates a better scalability for the online algorithm.

Figure 4 plots the learning objective, which exhibits similar trends. Lower values of α enable faster optimization. However, the difference in quality is less contrasted, as there is not a pronounced gap between the learning objectives for different values of α . We hypothesize that this effect is because the model can use a different MRF structure to mimic the data distribution. Experiments on held-out testing data presented in Figure 5 show that there is a positive correlation between the learning objective and the test negative log pseudo-likelihood, which confirms that the learned models do not over-fit the data even with small values of α . This result suggests that, while higher values of α help to recover the true structure, if the sole goal of learning the MRF structure is to produce a good generative model, then lower values of α can be used to speed up learning with only a small loss in quality. The first-hit baseline reaches the maximum number of added edges faster. However, it results in slower overall convergence in Figure 2 and a poor qualitative and quantitative behavior as seen in Figures 3 and 4, since it adds poor-quality edges.

In the smaller graphs, edge grafting has the advantage that its greedy search for the worst-violating edge enables large improvements in the objective. However, in the larger graphs, even though edge grafting precomputes sufficient statistics, the $O(n^2)$ cost of the greedy search causes its objective to descend at a slower rate than the online variants, which avoid this exhaustive search.

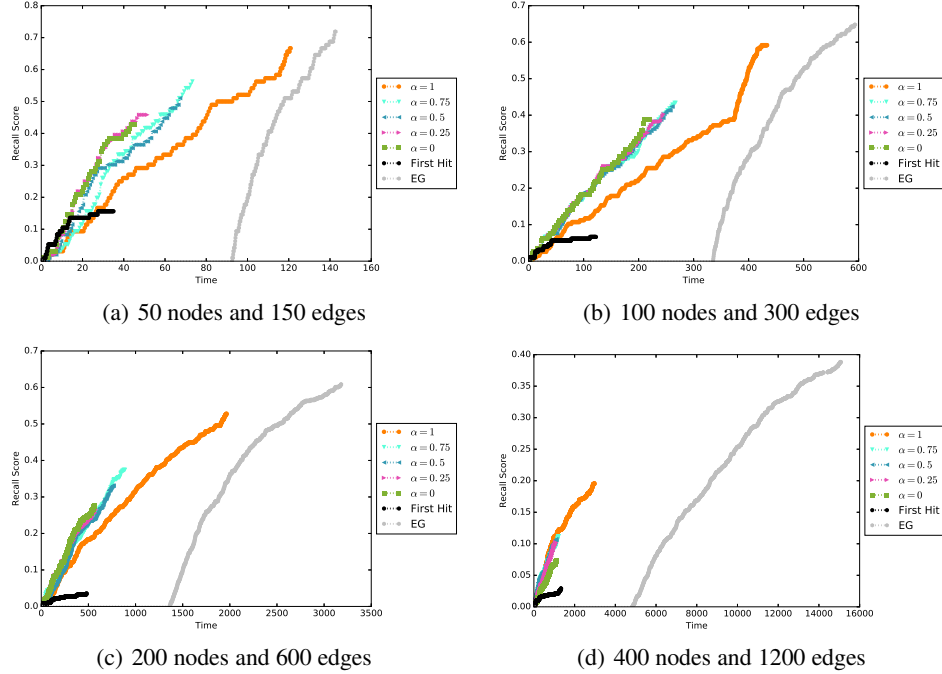


Figure 3: Recall vs. time (seconds) for varying MRFs sizes with $O(n)$ edges.

To evaluate the effectiveness of structure heuristics, Figure 6 plots the edge recall, for a limited number of activated edges, with and without the structure-based priority queue reorganization. The significant gap between the recall curves shows that they produce a higher-quality edge stream from the priority queue, resulting in a higher-quality reservoir and more relevant edges to activate.

4.2 Real data

We use three datasets: USDA plants [4],¹ Jester,² and Yummly recipes.³ The plants dataset comprises 34,781 plants with 68 different locations in the world. We treat plants as instances and locations as binary variables, leading to 9,248 parameters. The Jester dataset is a joke ratings dataset containing 100 jokes and 73,421 user ratings. We use jokes as variables and user ratings as instances. We map the ratings interval from a continuous interval in $[0, 20]$ to a discrete interval from 1 to 5, leading to 124,250 parameters. We sample 10,000 recipes from the Yummly dataset. We treat each of the 153 most common ingredients as a binary variable and consider each recipe a data instance, leading to 36,450 parameters.

Figures 7 and 8 show a positive correlation between the minimization of the learning objective and the testing negative log pseudo-likelihood. The results are similar to those from the synthetic experiments, where online edge grafting converges faster than edge grafting, and smaller values of α result in a faster convergence. The different-sized datasets illustrate the higher scalability of online edge grafting, as its improvement in convergence time over edge grafting increases with larger datasets.

5 Conclusion

We presented online edge grafting, a method based on a group- ℓ_1 formulation and online reservoir sampling. This incremental method activates edges instead of features and uses a reservoir to approximate greedy activation. Theoretical analysis shows that the method provides higher scalability than

¹<http://archive.ics.uci.edu/ml/datasets/Plants>

²<http://goldberg.berkeley.edu/jester-data/>

³<http://kaggle.com/c/whats-cooking>

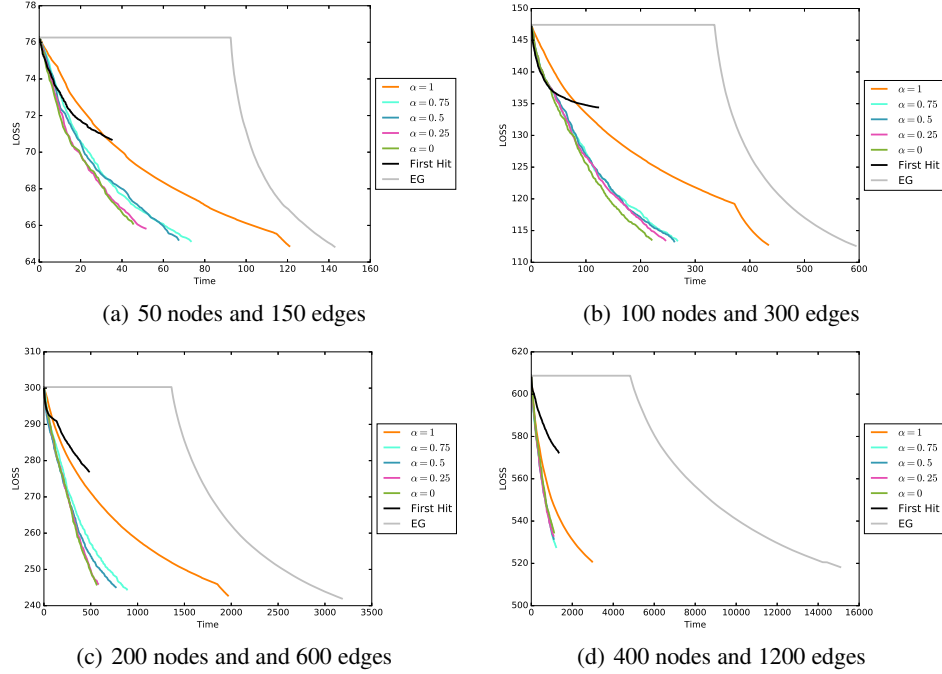


Figure 4: Loss vs. time (seconds) for varying MRFs sizes with $O(n)$ edges.

exhaustive edge grafting by avoiding its major bottlenecks. Experiments on synthetic and real data demonstrate that online edge grafting yields faster convergence on multiple datasets while producing a good structure recovery and a predictive ability similar to the costly exhaustive edge grafting method.

References

- [1] R. Albert and A. L. Barabási. Statistical mechanics of complex networks. *Reviews of modern physics*, 74(1):47, 2002.
- [2] G. Andrew and J. Gao. Scalable training of L1-regularized log-linear models. In *Proceedings of the 24th International Conference on Machine Learning*, pages 33–40. ACM, 2007.
- [3] J. Besag. Efficiency of pseudolikelihood estimation for simple Gaussian fields. *Biometrika*, 64(3):616–618, 1977.
- [4] W. Hämmäläinen and M. Nykänen. Efficient discovery of statistically significant association rules. In *Proceedings of the Eighth IEEE International Conference on Data Mining (ICDM)*, pages 203–212. IEEE, 2008.
- [5] A. T. Ihler, W. F. John III, and A. S. Willsky. Loopy belief propagation: Convergence and effects of message errors. *Journal of Machine Learning Research*, 6(May):905–936, 2005.
- [6] D. Koller and N. Friedman. *Probabilistic Graphical Models: Principles and Techniques*. MIT Press, 2009.
- [7] V. Kolmogorov. Convergent tree-reweighted message passing for energy minimization. *IEEE Transactions on Pattern Analysis and Machine Intelligence*, 28(10):1568–1583, 2006.
- [8] S.-I. Lee, V. Ganapathi, and D. Koller. Efficient structure learning of markov networks using l1-regularization. In *Advances in Neural Information Processing Systems*, pages 817–824, 2006.

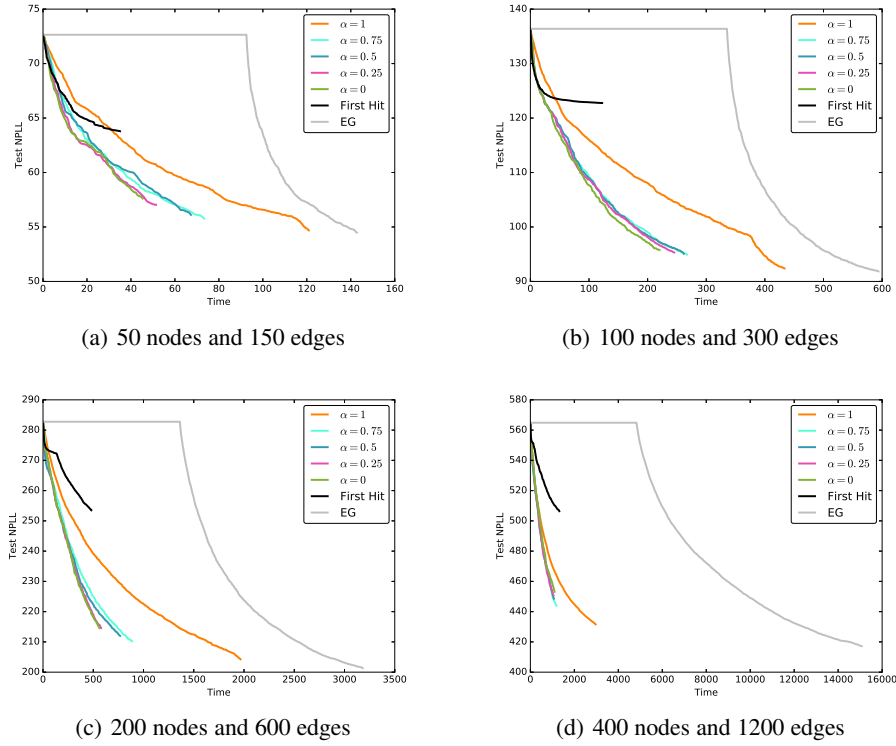


Figure 5: Negative log pseudo-likelihood vs. time (seconds) for varying MRFs sizes with $O(n)$ edges.

- [9] H. Liu and J. Zhang. Estimation consistency of the group lasso and its applications. In *Proceedings of the 12th International Conference on Artificial Intelligence and Statistics (AISTATS)*, 2009.
- [10] T. Meltzer, A. Globerson, and Y. Weiss. Convergent message passing algorithms: a unifying view. In *Proceedings of the Twenty-Fifth Conference on Uncertainty in Artificial Intelligence*, pages 393–401. AUAI Press, 2009.
- [11] K. P. Murphy, Y. Weiss, and M. I. Jordan. Loopy belief propagation for approximate inference: An empirical study. In *Proceedings of the Fifteenth Conference on Uncertainty in Artificial Intelligence*, pages 467–475. Morgan Kaufmann Publishers Inc., 1999.
- [12] F. Olken and D. Rotem. Random sampling from databases: a survey. *Statistics and Computing*, 5(1):25–42, 1995.
- [13] J. Pearl. *Probabilistic Reasoning in Intelligent Systems: Networks of Plausible Inference*. Morgan Kaufmann, 2014.
- [14] S. Perkins, K. Lacker, and J. Theiler. Grafting: Fast, incremental feature selection by gradient descent in function space. *Journal of Machine Learning Research*, 3:1333–1356, 2003.
- [15] P. van Emde Boas, R. Kaas, and E. Zijlstra. Design and implementation of an efficient priority queue. *Mathematical Systems Theory*, 10(1):99–127, 1976.
- [16] M. J. Wainwright and M. I. Jordan. Graphical models, exponential families, and variational inference. *Foundations and Trends in Machine Learning*, 1(1–2):1–305, 2008.
- [17] J. Zhu, N. Lao, and E. P. Xing. Grafting-light: fast, incremental feature selection and structure learning of Markov random fields. In *Proceedings of the 16th ACM SIGKDD International Conference on Knowledge Discovery and Data Mining*, pages 303–312. ACM, 2010.
- [18] H. Zou and T. Hastie. Regularization and variable selection via the elastic net. *Journal of the Royal Statistical Society: Series B (Statistical Methodology)*, 67(2):301–320, 2005.

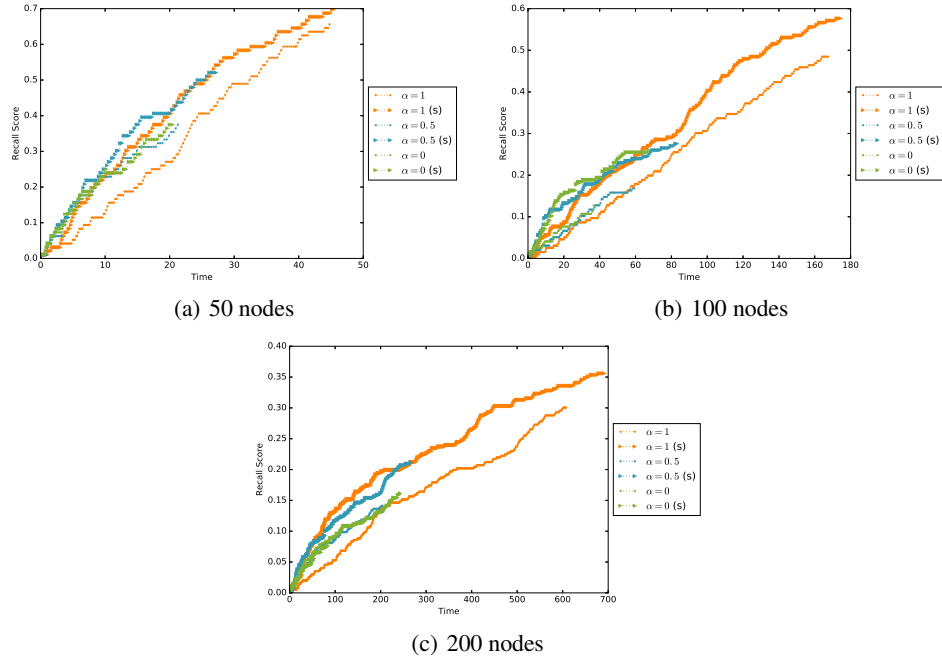


Figure 6: Role of structure heuristics in improving the quality of the learned MRF over training time (seconds). The proposed heuristics (labeled as ‘s’) produce higher recall for different MRF sizes.

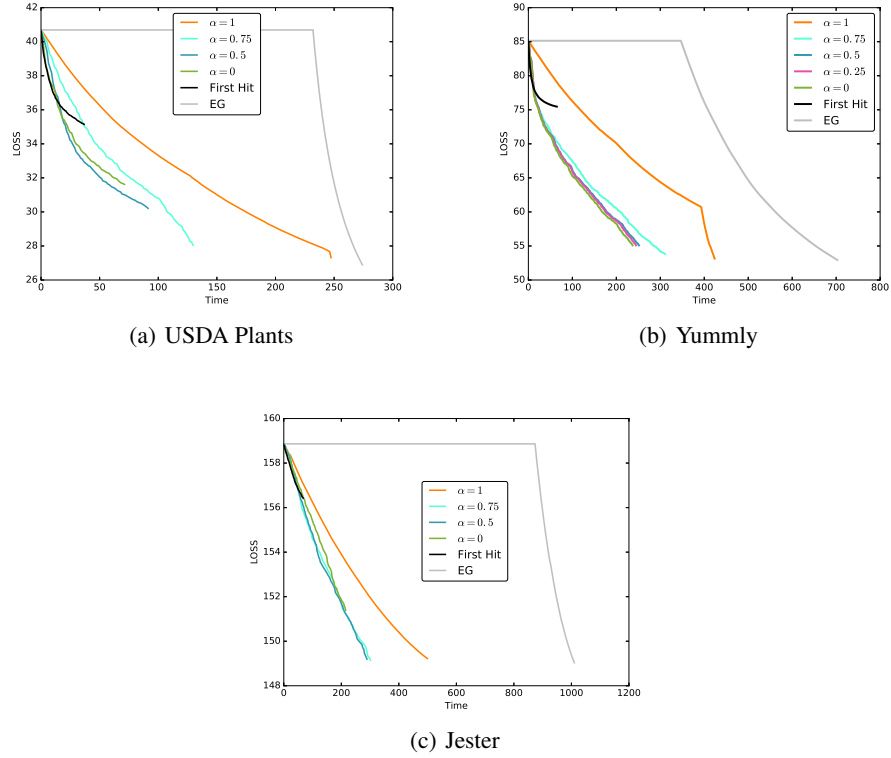
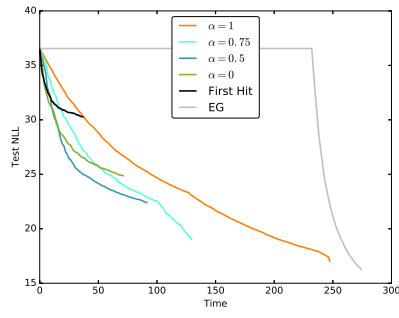
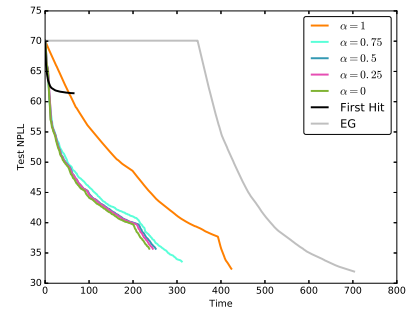


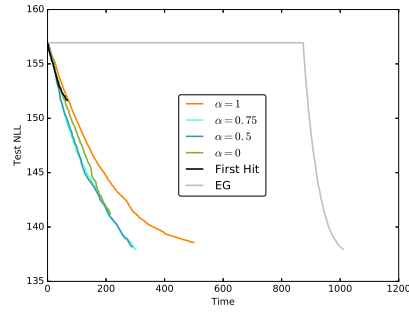
Figure 7: Learning objective for real data.



(a) USDA Plants



(b) Yummly



(c) Jester

Figure 8: Negative log pseudo-likelihood vs. seconds for real data.